

Evolution of low-mass stars and substellar objects. Contribution to the Galactic mass budget

G. Chabrier¹, I. Baraffe¹, F. Allard¹, and P.H. Hauschildt²

¹ Centre de Recherche Astrophysique de Lyon (UMR CNRS 5574),
Ecole Normale Supérieure de Lyon, 69364 Lyon Cedex 07, France

² Dpt. of Physics & Astronomy, University of Georgia, Athens, GA 30602, USA

Abstract. We briefly summarize our present knowledge of the theory of low-mass stars and substellar objects and their contribution to the Galactic population.

1 Introduction

The search for substellar objects (SSO) has bloomed over the past few years with the unambiguous identification of several free floating brown dwarfs (BDs) and with the discovery of numerous planets orbiting stars outside the solar system. Substellar objects therefore exist and ongoing and future observational projects are likely to reveal dozens more of such objects. Two groups, the Lyon group and the Tucson group, have aspired to derive a complete theory of the evolution and the spectral signature of low-mass, dense objects, from Sun-like to Saturn-like masses, covering 3 orders of magnitude in mass and 9 in luminosity, bridging the gap between stars and gaseous planets (see e.g. Burrows *et al.*, 1997 and Baraffe *et al.*, 1998 and references therein). These two groups have incorporated the best possible physics aimed at describing the mechanical and thermal properties of these objects - equation of state, synthetic spectra, non-grey atmosphere models. Both groups have "met in the middle" by successfully identifying the main spectral properties of the benchmark BD Gl229B, providing a determination of its mass and age (Marley *et al.*, 1996; Allard *et al.*, 1996). We refer to the afore-mentioned papers and the references therein for a complete description of the physics entering these models. Only a brief outline of these characteristics is given below.

2 The physics of sub-stellar objects

2.1 Interior

Central conditions for SSOs are typically $T_c \lesssim 10^5$ K and $\rho_c \sim 10^2\text{-}10^3$ g cm⁻³, characterizing a strongly coupled electron-ion plasma. Moreover, in the envelope, the electron binding energy is of the order of the Fermi energy

$Ze^2/a_0 \sim E_F$ so that *pressure-dissociation* and ionization take place along the interior. Very recently laser-driven shock wave experiments at Livermore have achieved pressures on liquid D_2 of up to 5 Mbar at high temperature (Collins *et al.*, 1998), exploring for the first time the regime of pressure-dissociation and ionization, therefore probing the equation of state (EOS) under conditions characteristic of SSO interiors. As shown in Figure 3 of Collins *et al.*, the experimental hugoniot revealed the excellent behaviour of the EOS developed by Saumon and Chabrier (Saumon *et al.*, 1995 and references therein). In particular the pronounced compressibility observed in the dissociation domain ($\rho/\rho_0 = 5.88$) agrees remarkably well with the theoretically predicted value. These experiments open a new window in physics and astrophysics by constraining the physics of the interior of SSOs in laboratory experiments.

2.2 Atmosphere

In the atmosphere, the hydrostatic equilibrium condition $d\tau = \bar{\kappa}dP/g$, where $g = Gm/R^2 \approx 10^3\text{-}10^5 \text{ cm s}^{-2}$ is the characteristic surface gravity of SSOs, yields $P_{ph} \sim g/\bar{\kappa} \approx 0.1\text{-}10 \text{ bar}$ and $\rho_{ph} \approx 10^{-6}\text{-}10^{-4} \text{ g cm}^{-3}$ at the photosphere. Collisional effects are important under such conditions and introduce sources of absorption like e.g. the collision-induced absorption (CIA) between H_2 - H_2 or H_2 -He below $\sim 5000 \text{ K}$ (see e.g. Borysow *et al.*, 1985). In the effective temperature range characteristic of low-mass stars (LMS) and SSOs ($T_{\text{eff}} \lesssim 5000 \text{ K}$), numerous molecules form, in particular metal oxydes and hydrides (TiO, VO, FeH, CaH), the major absorbers in the optical, and CIA H_2 , H_2O , CO which dominate in the infrared (see Allard *et al.*, 1997 for a review). The situation becomes even more complicated for SSOs, due to the changes in molecular chemistry which occur across the atmospheric temperature range from 2000 K (the coolest stars) to 170 K (jovian conditions). At 2000 K, most of the carbon is locked into carbon monoxide CO, while the oxygen is found in water vapor H_2O , dominantly, and in titanium TiO and vanadium VO monoxides. Below $\sim 1800 \text{ K}$, the dominant equilibrium form of carbon is no longer CO but CH_4 (Fegley & Lodders, 1996). As confirmed by the observation of Gl229B (Oppenheimer *et al.*, 1995), methane features begin to appear in the infrared while titanium dioxide and silicate clouds form at the expense of TiO, modifying profoundly the opacity of the atmosphere. For jovian-like atmospheres, the dominant equilibrium form of nitrogen is NH_3 ($T_{\text{eff}} \lesssim 600 \text{ K}$) and below $T_{\text{eff}} \sim 200 \text{ K}$ water condenses to clouds at or above the photosphere. As shown by Tsuji *et al.* (1996) and Jones & Tsuji (1997), there is evidence for condensation of metals and silicates into grains (e.g. TiO into $CaTiO_3$, Mg, Si into $MgSiO_3$) for $T_{\text{eff}} \lesssim 3000 \text{ K}$, i.e. at the bottom of the main sequence.

A proper inclusion of this complex atmospheric chemistry, and of a proper calculation of unknown cross-sections, represent the main challenge for a correct description of the spectral signature and the evolution of substellar ob-

jects. This grain formation process has been included in the calculations of the Tucson group only in term of condensation. The species are precipitated according to their condensation curves. If a species has condensed, it is left at its saturated vapor pressure (Burrows *et al.*, 1997). There is no inclusion of the radiative transfer effect of the grains. These models can thus be considered as grainfree opacity models. Recently, the Lyon group has extended similar calculations by implicitly including all condensed species into the radiative transfer equations (see Allard & Hauschildt, these proceedings). The atmosphere profiles were matched with the interior profiles at an optical depth deep enough to lie on the internal adiabat (see Chabrier & Baraffe, 1997).

3 Color-magnitude diagram

The present evolutionary calculations have been conducted with three different atmosphere models: (i) for hot objects, i.e. massive or young enough, to preclude the formation of grains ($T_{\text{eff}} \gtrsim 2800$ K), we have used the most recent grainless NGEN atmosphere models (Hauschildt *et al.*, 1999); (ii) for objects in the range 3000-1000 K, i.e. from the bottom of the MS down to Gliese229B-like objects, we have used complete atmosphere models which include the grain opacity sources in the transfer equations, the so-called DUSTY models (Allard & Hauschildt, these proceedings); (iii) for objects below 3000 K down to jovian temperatures, we have also considered cases where the condensates settle rapidly below the photosphere and - although modifying the atmosphere EOS - do not participate to the opacity, the so-called COND models. This is similar to the Burrows *et al.* (1997) calculations and is motivated by the relative absence of grain features in the atmosphere of objects below $T_{\text{eff}} \sim 1000$ K, i.e. Gliese229B-like and cooler objects. We found the effect of grain opacity (DUSTY) to affect only moderately the H-burning minimum mass. Models with grainless atmosphere yield $m = 0.072 M_{\odot}$, $L = 5 \times 10^{-5} L_{\odot}$ and $T_{\text{eff}} = 1700$ K at the H-burning limit, whereas models with grain opacity give $m \approx 0.07 M_{\odot}$, $L \approx 4 \times 10^{-5} L_{\odot}$ and $T_{\text{eff}} \approx 1600$ K, for solar composition.

Figure 1 displays a K vs J-K color-magnitude diagram (CMD). In terms of colors there is a competing effect between grain and molecular opacity sources for objects at the bottom and just below the MS. As already identified for e.g. Gl229B (Allard *et al.*, 1996; Marley *et al.*, 1996) CH_4 and CIA of H_2 lead to bluer infrared colors for SSOs, as illustrated by the NEG and COND models, whereas grain opacity results in a severe redening. Indeed, the present DUSTY models reproduce the spectra of the DENIS objects (Tinney *et al.*, 1998) and of the long puzzling object GD165B, which lies at the very edge of the H-burning limit (Kirkpatrick *et al.*, 1999). As T_{eff} decreases, grains settle below the photosphere and the DUSTY track will merge with the COND tracks. Observations of objects in the region between

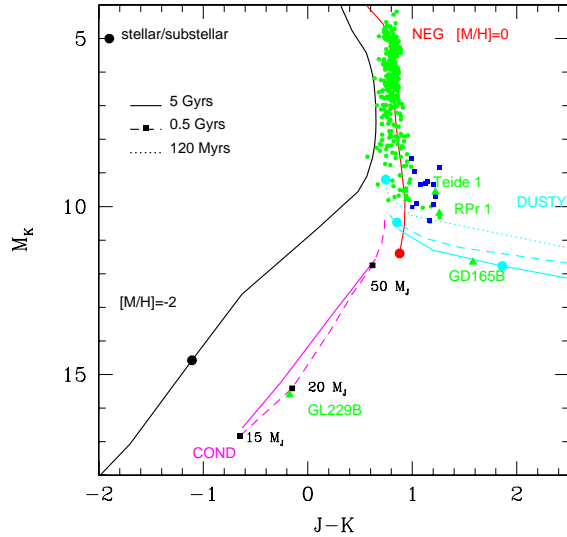


Fig. 1. M_K vs $(J-K)$ diagram for 3 isochrones, namely 5×10^9 yrs, 5×10^8 yrs and 1.2×10^8 yrs (the age of the Pleiades). The small circles and squares correspond to the observation of main sequence stars (Leggett, 1996) and of Pleiades objects (Bouvier *et al.*, 1998), respectively. Some identified BDs are also indicated

these two extreme cases will be the next confirmation of the present theory. In spite of this strong absorption in the IR, however, BDs around 1500 K radiate nearly 90% (99% with dust) of their energy at wavelengths longward of $1 \mu\text{m}$ and infrared colors are still preferred to optical colors (at least for solar metal abundance), with M, L, K as the favored bands, and $M_M \sim M_L \sim 11$, $M_K \sim 12$ at the H-burning limit, at 5 Gyr. Direct observation of the characteristic fluxes of SSO's are now within reach with several observational projects, like SOFIA, SIRTF, ISAAC (Burrows *et al.*, 1997; Allard & Hauschildt, these proceedings).

Several BD surveys are presently conducted in young clusters and it is important to develop accurate (non-grey) models for pre-MS stars and young BD's. The more massive of such objects will be hot enough so that grain formation does not occur, but for $t \lesssim 5 \times 10^7$ yrs, proper evolutionary calculations must consider two effects : (i) first of all the influence of the initial conditions must be carefully examined because they will significantly affect the mass-magnitude relationship; (ii) for young objects, the gravity is small ($\log g \lesssim 3$) and sphericity effects in the resolution of the transfer equations

might come into play. The derivation of such complete models is under work, but Figure 2 displays the present pre-MS models (Baraffe *et al.*, 1998) based on non-grey plane-parallel atmosphere models in a theoretical HR diagram.

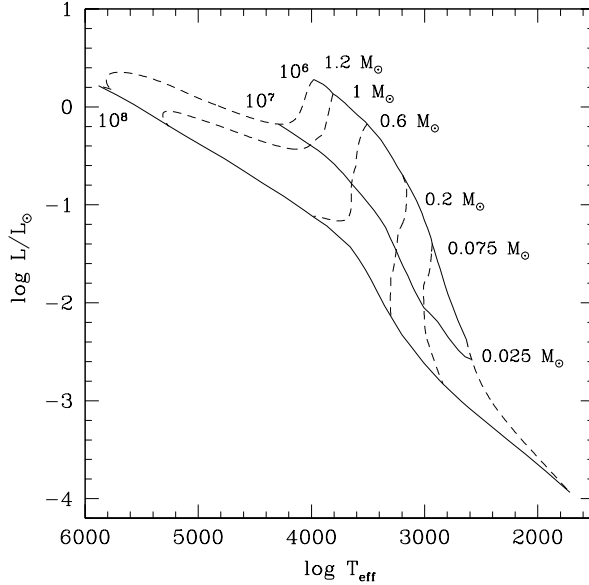


Fig. 2. Pre-main sequence isochrones (models are available from ftp site - see at the end of the paper)

4 Stellar and brown dwarf mass functions

4.1 Stellar mass function

The determination of the contribution of LMS and SSOs to the Galactic mass budget requires the correct determination (slope and normalization) of the mass-function (MF) down to the hydrogen burning limit, in order to have a solid foundation for extrapolation into the substellar domain. This issue, however, is presently not completely settled for the Galactic disk, and significant differences exist between the MF inferred from parallax-determined luminosity functions (LF) (Kroupa, 1995) and from the HST photometric LF (Gould, Flynn & Bahcall, 1997) (see Méra, Chabrier & Schaeffer, 1998, Fig. 1). It is relatively safe to say, however, that the MF keeps rising down to the H-burning limit, although with a slope shallower than a

Salpeter MF. The LMS ($m \leq 0.6 M_{\odot}$) mass densities inferred from the integration of the two afore-mentioned MFs (nearby and HST) yield, respectively, $\rho_{LMS} \approx (1.9 \pm 0.1) \times 10^{-2}$ and $\rho_{LMS} \approx (2.6 \pm 0.2) \times 10^{-2} M_{\odot} pc^{-3}$ (Méra *et al.*, 1998). Adding up the contribution from more massive stars and stellar remnants yields $\rho_{\star} \approx (4.0\text{--}4.6) \pm 0.3 \times 10^{-2} M_{\odot} pc^{-3}$ in the Galactic disk, i.e. a surface density $\Sigma_{\star} \approx 31 \pm 2 M_{\odot} pc^{-2}$. This corresponds to a stellar *number*-density $n_{\star} \sim 0.06$ (HST) and $\sim 0.35 pc^{-3}$ (nearby).

For the spheroid the question is more settled with a MF with $\alpha \lesssim 1$ (where $dN/dm \propto m^{-\alpha}$) and a stellar density $\rho_{\star} < 4.0 \times 10^{-5} M_{\odot} pc^{-3}$, less than 1% of the required dynamical density (Graff & Freese, 1996; Chabrier & Méra, 1997; Gould *et al.*, 1998), i.e. a number density $n_{\star} < 10^{-3} pc^{-3}$. Extrapolating into the BD domain yields for the spheroid $n_{BD} < 10^{-4} pc^{-3}$, $\rho_{BD} < \rho_{\star}/10$, i.e. a microlensing optical depth $\tau \sim 10^{-9}$, about 1% of the value measured toward the LMC. The puzzle remains unsolved for the *dark halo* MF, although both the HDF observations and the narrow-range of the observed time-distribution of the microlensing events towards the LMC strongly suggest an IMF different from a Salpeter one below $\sim 1 M_{\odot}$ (see e.g. Chabrier, 1999).

4.2 Brown dwarf mass function

A proper census of the number of brown dwarfs ($m < 0.07\text{--}0.09 M_{\odot}$, depending on the metallicity) has significant implications for our understanding of how stars and planets form. The determination of the BD MF is a complicated task. By definition BDs never reach thermal equilibrium and most of the BD's formed at the early stages of the Galaxy will have fainted to very low-luminosities ($L \propto 1/t$, see e.g. Burrows & Liebert, 1993). Thus observations will likely be biased towards young and massive BD's. The age uncertainty is circumvented when looking for the BD MF in stellar clusters since objects in that case are likely to be coeval. The Pleiades cluster has been extensively surveyed and several BDs have been identified down to $\sim 25 M_J$ (Martin *et al.*, 1998; Bouvier *et al.*, 1998). A single power-law function from ~ 0.4 to $0.04 M_{\odot}$ seem to adequately reproduce the observations with some remaining uncertainty in the exponent $\alpha \sim 0.6 - 1.0$ (Bouvier *et al.*, 1998; Martin *et al.*, 1998). By examining the various observations of Doppler radial velocity surveys, Basri and Marcy (1997) reach the conclusion that all data are consistent with $0 \lesssim \alpha \lesssim 1$ (see Basri, these proceedings for an updated analysis of such data). On the other hand Mayor *et al.* (1997) find for the mass function of the companions of the G and K dwarf sample observed with CORAVEL a power-law function with $\alpha \sim 0.4$ from 0.4 down to $0.005 M_{\odot}$. The determination of the MF in young clusters is potentially very interesting. Indeed young clusters did not have time to experience evaporation in the outer regions or mass segregation in the central regions and the present-day MF should reflect relatively closely the initial MF. Such a MF determination, however, is hampered by two observational and theoretical problems. From the observational point of view, young objects are immersed into dust and a proper

determination of the LF requires a correct determination of the *differential* reddening in the cluster. From the theoretical point of view, none of the MFs determined up to now in young clusters include a careful examination of the effects mentioned in §3 (initial conditions, sphericity, non-grey effects) and thus are of dubious validity. It is thus certainly premature to claim a robust determination of the MF in young clusters.

An independent, powerful information on the stellar and substellar MF comes from microlensing observations. Indeed, the time distribution of the events provides a (although model-dependent) determination of the mass distribution and thus of the minimum mass of the dark objects: $dN_{ev}/dt_e = E \times \epsilon(t_e) \times d\Gamma/dt_e \propto P(m)/\sqrt{m}$, where E is the observed exposure, i.e. the number of star×years, ϵ is the experimental efficiency, Γ is the event rate and $P(m)$ is the mass probability distribution. The analysis of the published 40 MACHO + 9 OGLE events towards the bulge is consistent with a rising mass function at the bottom of the MS with a minimum mass $m_{inf} \sim 0.05 M_\odot$, whereas a decreasing MF below $0.2 M_\odot$ is excluded at the 95% confidence level (Han & Gould, 1995; Méra *et al.*, 1998). Although the time distribution might be affected by various biases (e.g. blending) and robust conclusions must await for larger statistics, the present results suggest that in order to explain both star counts and the microlensing experiments, a substantial amount of SSOs must be present in the galactic disk. Indeed, extrapolation of the stellar MF (§4.1) into the BD domain down to $0.05 M_\odot$ yields for the Galactic disk $\rho_{BD} \sim 4.0 \times 10^{-3} M_\odot pc^{-3}$, i.e. $\Sigma_{BD} \approx 3 M_\odot pc^{-2}$, i.e. a BD *number-density* comparable to the stellar one, $n_{BD} \sim 0.1 pc^{-3} \sim n_\star$.

For the spheroid, extrapolation of the afore-mentioned stellar MF yields $\rho_{BD} \lesssim 10^{-5} M_\odot pc^{-3}$, $n_{BD} \lesssim 10^{-4} pc^{-3}$, whereas for the dark halo the normalization is about 2 orders of magnitude smaller (Chabrier & Méra, 1997).

4.3 Planet mass function

It is obviously very premature to try to infer the mass distribution of exoplanets. This will first require a clear, both theoretical and observational, distinction between planets and brown dwarfs. An interesting preliminary result, however, comes from the observed mass distribution of the secondaries conducted by Mayor and collaborators. As shown by Mayor *et al.* (1997), there is a strong discontinuity in the mass distribution at $m_2/\sin i \approx 5 M_J$, with a clear peak below this limit. If confirmed this would suggest that planet formation in a protoplanetary disk is a much more efficient mechanism than BD formation, which results from cloud collapse and fragmentation.

5 Conclusion and perspectives

As mentioned in the introduction, accurate models for low-mass stars, brown dwarfs and giant planets are needed to shed light on the observable properties

of these objects and to provide guidance to the ongoing and future surveys aimed at revealing their contribution to the Galactic population. From this point of view, tremendous progress has been made in the recent years with the derivation of consistent evolutionary model and synthetic spectra calculations which accurately reproduce the observed sequences of globular clusters, Pleiades, field objects and of the benchmark BD Gl229B in *various photometric passbands* (see references mentioned in the Introduction). Moreover the afore-mentioned LMS models have been shown to accurately reproduce the observational mass-magnitude relationship (Henry & McCarthy, 1993; Henry *et al.*, 1999) both in the optical and in the infrared (Baraffe *et al.*, 1998) and to yield a consistent, coeval sequence for the quadruple system *GG-Tau*, whose component masses extend from $1.2 M_{\odot}$ down to $\sim 0.035 M_{\odot}$ (White *et al.*, 1999), a formidable test for the theory. On the other hand, stringent constraints on the theory of dense/cool objects are now provided by laboratory high-pressure experiments, for the interior, and by various spectroscopic and photometric observations of LMS and SSO's. Any theory aimed at describing the mechanical and thermal properties of these objects *must* be confronted to these experimental/observational constraints in order to assess any degree of validity. Improvement in the theory will proceed along with the discovery of many more SSO's, hopefully bridging the gaps on either side of Gl229B from the bottom of the MS to Jupiter-like objects. Observation of a transit EGP would allow the determination of the radius and the mass of the object, providing a formidable constraint on the theory. For 51-Peg-like objects, the probability to observe such a transit $p = d_{\star}/D$, where d_{\star} and D are the stellar and orbital diameters, respectively, is $p \sim 10\%$, by no means negligible.

The increasing number of observed LMS and SSOs, together with the derivation of accurate models, will allow eventually a robust determination of the stellar and substellar mass functions, and thus of the exact density of these objects in the Galaxy. As discussed in §4, present MF determinations in various Galactic regions point to a slowly rising MF near and below the H-burning limit, with a BD number density comparable to the stellar one. Whether this behaviour is universal (although we already know it is certainly not the case for the dark halo), whether it is consistent with a general log-normal form, must await confirmation from future observations. On the other hand, the amazingly rapid pace of exoplanet discoveries should yield the determination of the planetary MF. These combined informations will allow the determination of the BD minimum mass and planet maximum mass.

As seen, the physics of SSOs involves an amazingly large domain of physics and astrophysics, from the fundamental N-body problem to star formation and Galactic evolution, and will certainly remain a lively domain of the early 21st century astronomy.

The present grainless models are available from:

```
ftp ftp.ens-lyon.fr, username: anonymous
ftp > cd /pub/users/CRAL/ibaraffe
```

ftp > get BCAH98_models and BCAH98_models_BD

References

1. Allard, F., Hauschildt, P.H., Alexander, D., & Starrfield, S. 1997, *ARA&A*, **35**, 137
2. Allard, F., Hauschildt, P.H., Baraffe, I., & Chabrier, G., 1996, *ApJ*, **465**, L123
3. Baraffe, I., Chabrier, G., Allard, F. and Hauschildt, P.H., 1998, *A&A*, **337**, 403
4. Basri, G., & Marcy, G., 1997, *AIP Conf. Ser.*, **393**, 228
5. Borysow, A., Trafton, L., Frommhold, L. & Birnbaum, G., 1985, *ApJ*, **296**, 644
6. Bouvier, J., Stauffer, J.R., Marin, E.L., Barrado Y Navascues, D., Wallace, B., & Bejar, V.J.S., 1998, *A&A*, **336**, 490
7. Burrows A., Marley, M., Hubbard, W.B., Lunine, J.I., Guillot, T., Saumon, D., Freedman, R., Sudarsky, D., Sharp, C. 1997, *ApJ*, **491**, 856
8. Burrows A., & Liebert, J., 1993, *Rev. Mod. Phys.*, **65**, 301
9. Chabrier, G., 1999, *ApJ*, **513**, L103
10. Chabrier, G., and Méra, D., 1997, *A&A*, **328**, 83
11. Chabrier, G. and Baraffe, I., 1997, *A&A*, **327**, 1039
12. Collins, G.W., *et al.*, 1998, *Science*, **281**, 1178
13. Fegley B., & Lodders K., 1996, *ApJ*, **472**, L37
14. Gould, A., Flynn, C., and Bahcall, J., 1998, *ApJ*, **503**, 798
15. Graff, D. and Freese, K., 1996, *ApJ*, **456**, L49
16. Han, C. and Gould, A., 1995, *ApJ*, **447**, 53
17. Hauschildt, P.H., Allard, F., Baron, E., 1999, *ApJ*, **512**, 377
18. Henry, T., & McCarthy, D.W., 1993, *AJ*, **106**, 773
19. Henry, T., *et al.*, 1999, *ApJ*, **512**, 864
20. Jones, H., & Tsuji, T., 1997, *ApJ*, **480**, L39
21. Kirkpatrick, J. D., Allard, F., Bida, T., Zuckerman, B., Becklin, E.E., Chabrier, G., and Baraffe, I., 1999, *ApJ*, in press
22. Kroupa, P., 1995, *ApJ*, **453**, 358
23. Leggett, S.K., Allard, F., Berrieman, G., Dahn, C.C. & Hauschildt, P.H., 1996, *ApJS*, **104**, 117
24. Marley, M.S., Saumon, D., Guillot, T., Freedman, R., Hubbard, W.B., Burrows, A., Lunine, J.I. 1996, *Science*, **272**, 1919
25. Martin, E., Basri, G., Zapatero-Osorio, M.R., Rebolo, R., Lopez, R.J. Garcia, 1998, *ApJ*, **507**, L41
26. Mayor, M., Queloz, D., Udry, S., & Halbwachs, J-L., 1997, in *Rencontre de Blois*
27. Méra, D., Chabrier, G., and Schaeffer, R., 1998, *A&A*, **330**, 937
28. Oppenheimer, B.R., Kulkarni, S.R., Nakajima, T., Matthews, K. 1995, *Science*, **270**, 1478
29. Saumon, D., Chabrier, G., and VanHorn, H.M., 1995, *ApJS*, **99**, 713
30. Tinney, C., Delfosse, X., Forveille, T., & Allard, F., 1998, *A&A*, **338**, 1066
31. Tsuji, T., Ohnaka, K. and Aoki, W. 1996a, *A&A*, **305**, L1
32. Tsuji, T., Ohnaka, K., Aoki, W., Nakajima. T. 1996b, *A&A*, **308**, L29
33. White, R., Ghez, A., Reid, I., Schultz, G., 1999, *astro-ph/9902318*